

Effect of Strain History on Stress and Permanent Set in Cross-Linking Networks: A Molecular Dynamics Study

Dana R. Rottach

Department of Chemical & Nuclear Engineering, University of New Mexico, Albuquerque, New Mexico 87106

John G. Curro,* Gary S. Grest, and Aidan P. Thompson

Sandia National Laboratories, Albuquerque, New Mexico 87185

Received February 9, 2004; Revised Manuscript Received April 29, 2004

ABSTRACT: Polymer networks undergoing cross-linking reactions are studied using molecular dynamics simulations to investigate how the stress is influenced by the coupling between cross-linking and deformation. For networks cross-linked in the undeformed state, the modulus increases linearly with the cross-link density as expected from rubber elasticity theory. When cross-links are added to a network that was uniaxially deformed, the stress remains constant in accordance with the independent network hypothesis of Tobolsky. When the deformed network is subsequently released, permanent set is observed. Using the independent network hypothesis, together with the affine theory of rubber elasticity, a constitutive model is developed that accounts for the effect of the coupling between the cross-link density and strain histories of the network. The permanent set predictions from the affine model are higher than found from MD simulations.

I. Introduction

The properties of polymer networks can change with time because of viscoelastic relaxation due to motions of chains on a variety of time scales. Chemical reaction can also occur in most organic polymer networks at high temperatures, or long times, resulting in permanent changes in the network topology with attendant changes in the physical properties with time. On very long time scales the kinetics of these various reactions, rather than the viscoelasticity, frequently controls the time dependence of the macroscopic properties. Tobolsky,^{1,2} followed by Berry, Scanlan, and Watson,³ and Flory⁴ were the first to systematically study these “chemical relaxation” effects. Fundamentally different behavior results depending upon whether chemically induced chain scission or cross-linking occurs. Chemical scission of bonds causes the effective cross-link density of the network and the equilibrium rubber elastic modulus to decrease with time. Neglecting viscoelastic effects, the stress on a network undergoing scission reactions depends only^{1,5,6} on the current value of the cross-link density. By contrast, the stress on a network when additional cross-linking (e.g., postcuring) takes place depends not only on the current value of the cross-link density but also on the state of strain the sample^{1,2} was in when each cross-link was formed. One consequence of this cross-linking/strain history dependence is that the network can have a permanent set when the stress is removed. Problems of this type have been treated with a general constitutive model by Wineman et al.⁸ Recently, Mott and Roland⁹ performed birefringence measurements on networks cross-linked in unstrained and strained states. Santangelo and Roland¹⁰ studied the effect of cross-linking history on the strain crystallization and fatigue resistance of elastomeric materials. Despite the fact that chemical relaxation is very important where elastomers are used for extended periods of time or at high temperature, surprisingly little research has been carried out in this area. In this investigation

we employ molecular dynamics (MD) simulations to study the effect of cross-linking on the mechanical properties of elastomeric networks.

The complexity of the stress/strain properties of a cross-linking network can be illustrated by considering the following two experiments. First, consider a network well above the gel point, undergoing additional cross-linking reactions in the unstrained state. From rubber elasticity theory we expect that the equilibrium modulus would continue to increase linearly with the number of cross-links that form (neglecting the formation of elastically ineffective cross-links, e.g., rings). Now consider a uniaxial stress relaxation experiment in which additional cross-links are added to a strained network. Neglecting purely viscoelastic effects, how does the stress change as these new cross-links are added? Tobolsky argued² that as long as the network is held in the strained state, no change in stress should be detectable since the new network chains that form have their state of ease in the strained condition. With this hypothesis, Tobolsky constructed an “independent network” model to describe the permanent set that the network would experience when the stress is removed. Intermittent and continuous stress relaxation and permanent set experiments^{1,7} tend to support the validity of Tobolsky’s hypothesis.

It is difficult to carry out well-controlled chemical relaxation experiments on elastomeric networks for two reasons. First, it is hard to control the chemistry. Generally thermal or oxidative degradation leads to simultaneous scission and cross-linking, making it problematical to isolate one process from the other. Second, because networks are infusible and insoluble, it is very difficult to characterize network structure and any changes caused by chemical reaction. Very few characterization tools are available to monitor chemical degradation effects. Indeed, the stress relaxation behavior itself might be the most sensitive measure of any chemically induced changes in network structure. For

these reasons, it is advantageous to use computer simulation, rather than laboratory experiments, as a tool to study the behavior of polymer networks. Eichinger and co-workers used computer simulations to examine the gelation and topology of end-linked networks^{11–13} and random cross-linked systems.^{14,15} MD simulations have been used by Everaers and co-workers to test various rubber elasticity theories^{16–19} and by Grest and co-workers to study gelation and vulcanization²⁰ and probe viscoelastic relaxation processes in networks.^{21,22}

Our overall goal is to deduce an accurate constitutive model relating the stress to the strain and chemical reaction history of elastomeric networks. Earlier work^{5,6} addressed networks undergoing chain scission and led to a linear viscoelastic formulation of the constitutive equation. In the present investigation we focus on the more difficult problem of describing the constitutive model of a network undergoing cross-linking. To isolate the coupling between cross-linking and strain history, we only consider quasi-equilibrium conditions where viscoelastic contributions to the stress have mostly relaxed out. Furthermore, there are no scission reactions, and the only changes in the network structure arise from cross-linking events.

In this paper we first discuss the independent network hypothesis based on Tobolsky's original ideas.^{1,2} This is followed by a description of how MD simulations are used to study the cross-linking of polymers and stresses on the resultant networks. Results are then shown and discussed for networks cross-linked in the undeformed and deformed states, followed by simulations of permanent set.

II. Independent Network Model

For simplicity, in this work we will initially consider only one-dimensional, uniaxial strain. Generalization to arbitrary three-dimensional strain fields is straightforward^{3,4} but is not necessary to address the essential physics of the network. Tobolsky^{1,2} considered the case where an unstrained network, having ν_0 network chains, is uniaxially deformed from length L_0 to L_1 , while in the deformed state, additional network chains ν_1 are formed. Now consider what the stress would be on the network if the sample length is changed to L . Tobolsky argued that the network of constant volume V would behave like two independent networks: the original one having ν_0 cross-links and the strained one with ν_1 network chains. Using the affine model of rubber elasticity,²³ Tobolsky took the uniaxial stress σ to be the superposition of the contributions from the two independent networks:

$$\sigma = \frac{\nu_0 k_B T}{V} \left[\left(\frac{L}{L_0} \right)^2 - \left(\frac{L_0}{L} \right) \right] + \frac{\nu_1 k_B T}{V} \left[\left(\frac{L}{L_1} \right)^2 - \left(\frac{L_1}{L} \right) \right] \quad (1)$$

Although Tobolsky^{1,2} considered only two independent networks, it is straightforward to generalize his result for an arbitrary length history $L_0, L_1, L_2, \dots, L_n$.

$$\sigma = \frac{k_B T}{V} \sum_{i=0}^n \nu_i \left[\left(\frac{L}{L_i} \right)^2 - \left(\frac{L_i}{L} \right) \right] \quad (2)$$

where ν_i is the number of network chains added while the network length was L_i . Berry, Scanlan, and Watson³ and Flory⁴ demonstrated that the independent network

result in eqs 1 and 2 holds for Gaussian chains with the affine deformation assumption. Equation 2 can be generalized further to the case where the length $L(t)$ and number of network chains $\nu(t)$ vary continuously with time.

$$\sigma(t) = \frac{k_B T}{V} \int_{t_{\text{gel}}}^t \left[\left(\frac{L(t)}{L(s)} \right)^2 - \left(\frac{L(s)}{L(t)} \right) \right] d\nu ds \quad (3)$$

Since there are no elastically effective chains prior to gelation, we take $\nu(t)$ to include only those cross-links added after the gel point. Hence, the lower limit of the integral in eq 3 is the time t_{gel} required for gelation.

For a simple stress relaxation experiment, we have the strain history $L = L_0$ for $t_{\text{gel}} \leq t < t_0$ and $L = L_1$ for $t_0 \leq t < t_1$. For this case eq 3 becomes simply

$$\begin{aligned} \sigma(t) &= \frac{k_B T}{V} \left[\left(\frac{L_1}{L_0} \right)^2 - \left(\frac{L_0}{L_1} \right) \right] \int_{t_{\text{gel}}}^{t_0} d\nu ds \\ &= \frac{\nu_0(t) k_B T}{V} \left[\left(\frac{L_1}{L_0} \right)^2 - \left(\frac{L_0}{L_1} \right) \right] \end{aligned} \quad (4)$$

for times $t_0 \leq t < t_1$. Thus, neglecting viscoelastic effects, the time-dependent stress is predicted to depend only on the number of network chains $\nu_0(t)$ formed in the unstrained state. In general, ν_0 can decay with time for $t > t_0$ due to scission reactions, although in the present simulations chain scission does not occur. From eq 4 we see that a consequence of the independent network model is that even though additional cross-links $\nu_1(t)$ are being added to the strained network, they do not contribute to the stress during the interval $t_0 \leq t < t_1$ when the network is held at $L = L_1$. The $\nu_1(t)$ cross-links will come into play, however, if the length of the sample is changed further so that $L = L_s$ for $t \geq t_1$. Equation 3 now predicts that

$$\sigma(t) = \frac{\nu_0(t) k_B T}{V} \left[\left(\frac{L_s}{L_0} \right)^2 - \left(\frac{L_0}{L_s} \right) \right] + \frac{\nu_1(t) k_B T}{V} \left[\left(\frac{L_s}{L_1} \right)^2 - \left(\frac{L_1}{L_s} \right) \right] \quad (5)$$

In particular, if we set $\sigma(t) = 0$ for $t \geq t_1$, then we can obtain the permanent set of the network as the length L_s the sample will return to after the stress is removed from the sample. The permanent set, measured in the so-called compression set experiment, is often used in industry²⁴ as a figure of merit for the aging stability of rubber compounds. We define the permanent set as

$$P_s = \frac{L_s - L_0}{L_1 - L_0} = \frac{\lambda_s - 1}{\lambda_1 - 1} \quad (6)$$

where λ_s and λ_1 are the corresponding deformation ratios. From eq 5 the permanent set is predicted to be

$$P_s = \frac{\lambda_1 \left[\frac{\nu_1/\nu_0 + 1/\lambda_1}{\nu_1/\nu_0 + \lambda_1^2} \right]^{1/3} - 1}{\lambda_1 - 1} \quad (7)$$

for the independent network model where $\lambda_1 = L_1/L_0$ is a measure of the extent of strain during the set experiment. The purpose of this work is to test the independent network hypothesis. In particular, we will test both the stress relaxation and permanent set predictions in eqs 4 and 7 using MD simulations in

which the cross-link and strain variables can be precisely controlled.

It should be emphasized that we used the affine model of rubber elasticity in this independent network analysis. This is obviously an oversimplified theory. In particular, one could envision that the interplay between elastically effective and ineffective chains could complicate the response of the network as new cross-links are added, especially near the gel point. Other, more accurate, nonaffine rubber elasticity theories^{17,19} could, in principle, be employed in an analogous manner to the Tobolsky approach.

III. MD Simulations

Large-scale, MD simulations were performed in a NVT ensemble using the LAMMPS parallel MD code,²⁵ modified to incorporate chemical reactions. Typically 36–80 processors were used with a time step $\Delta t = 0.005\tau$, where $\tau = \sigma_{\text{LJ}}(m/\epsilon)^{1/2}$, m is the mass of a bead, and σ_{LJ} and ϵ are the Lennard-Jones parameters. The polymers were modeled using the standard bead–spring model²⁶ in which monomers interact with a truncated Lennard-Jones potential

$$V(r) = 4\epsilon \left[\left(\frac{\sigma_{\text{LJ}}}{r} \right)^{12} - \left(\frac{\sigma_{\text{LJ}}}{r} \right)^6 + \frac{1}{4} \right], \quad r \leq 2^{1/6}\sigma_{\text{LJ}}$$

$$= 0, \quad r > 2^{1/6}\sigma_{\text{LJ}} \quad (8)$$

An additional interaction between adjacent beads along a chain

$$V_{\text{ch}}(r) = -0.5k_{\text{B}}R_0^2 \ln[1 - (r/R_0)^2], \quad r \leq R_0$$

$$= \infty, \quad r > R_0 \quad (9)$$

and between cross-linked monomers is used to give chain connectivity. Here $R_0 = 1.5\sigma_{\text{LJ}}$ is the maximum extension of a bond and $k = 30\epsilon/\sigma_{\text{LJ}}^2$. We first equilibrated a melt of 500 chains, each having 500 monomers; periodic boundary conditions were employed with a density of $\rho\sigma_{\text{LJ}}^3 = 0.85$, $\sigma_{\text{LJ}} = 1$, and $kT_{\text{B}}/\epsilon = 1.27$. Four percent of the beads on each chain are randomly labeled as reactive sites, subject to the condition that the reactive sites are separated by at least two bonds.

After equilibration, the distances between all pairs of reactive sites are determined at time intervals of τ_x . Pairs of sites within a capture radius of $1.3\sigma_{\text{LJ}}$ are “bonded” with a probability q after which the MD simulation is continued. Initially the periodic box is cubic with sides L_0 . The network is deformed by changing the box length to λL_0 in the x direction and to $L_0/\sqrt{\lambda}$ in the y and z directions so the volume remains constant. This uniaxial deformation occurs over a time period of 16τ . The average stress σ in the x direction is obtained from the simulation as the deviatoric part of the stress tensor²⁸ $\sigma = (1 + \nu_{\text{P}})(P_{xx} - P) \approx 3(P_{xx} - P)/2$, where $P = \sum_i P_{ii}/3$ is the hydrostatic pressure. The factor in σ involving Poisson’s ratio ν_{P} is required because in our simulations the box is deformed at constant volume. For elastomeric materials Poisson’s ratio is very close to $1/2$.

IV. Results and Discussion

The cross-linked samples were prepared by turning on the cross-linking reactions until the sample is well above the gel point. The reaction rate was chosen to be small so that approximate quasi-equilibrium conditions

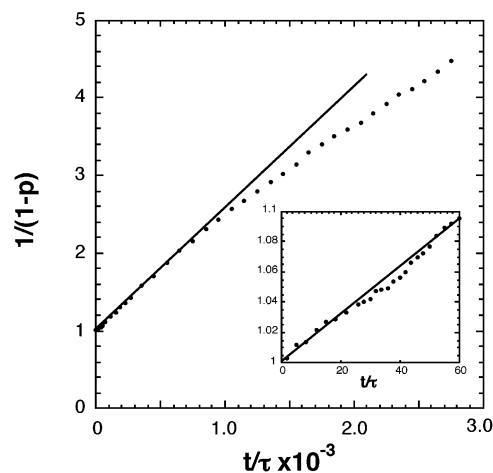


Figure 1. Fractional conversion of reactive sites p in the unstrained state. A straight line would be expected for a second-order kinetic process. The inset shows the early time reaction during the gelation.

were maintained during the gelation process. Control over the reaction rate, relative to the diffusion rate of the chains, was achieved through the variables τ_x , the time between reactions, and the acceptance probability, q . If the reactions are not diffusion-controlled, then we expect the cross-linking reactions occurring between reactive sites in our simulation to exhibit second-order reaction kinetics where $(1 - p)^{-1} \propto t$. p is the extent of conversion of reactive sites defined as $p = [n(0) - n(t)]/n(0)$, and $n(t)$ is the number of reactive sites remaining at time t . In our simulations we set $\tau_x = 10\tau$ and adjusted q in the range $10^{-5} - 10^{-3}$ so that second-order kinetics approximately holds during gelation, as can be seen from the inset in Figure 1. The gel point was estimated by identifying the conversion p_c where a cluster in the primary box first connects to its images in adjacent periodic boxes in all three spatial directions. The gel point for this particular sample was estimated to be $p_c \sim 0.096$ which occurred at $t = 59.5\tau$ after the cross-linking reactions were started. This gel point is consistent with the previous MD studies of gelation by Grest and Kremer²⁰ on finite size networks.

The cross-linking reaction kinetics is displayed at long times in the main part of Figure 1. It can be seen that second-order reaction kinetics hold out to approximately $t = 10^3\tau$, where $p \sim 0.60$. For higher conversions, the reactions start to become diffusion-controlled²⁹ as the mobility of the reactive sites becomes small as expected when the network continues to cure. In Figure 2 the sol fraction of the network near the gel point is plotted. It can be seen from this plot that the fraction of chains not connected to the network rapidly approaches zero above the gel point. By the time that the conversion has reached $p = 0.40$ in our sample, all the chains are part of the network and the sol fraction is zero. At this point the sample is taken to be representative of an elastomeric network and is the starting point for our test of the independent network approximation. The number of network chains depends on the conversion according to $\nu = (p - p_c)n(0)$. Because of the presence of intramolecular cross-links and other network imperfections,¹⁴ not all of these network chains will be elastically active.

We first examined the effect of “postcuring” on unstrained networks. Various MD runs were carried out where additional cross-linking reactions are allowed to occur, leading to samples between $p = 0.45$ and 0.85 .

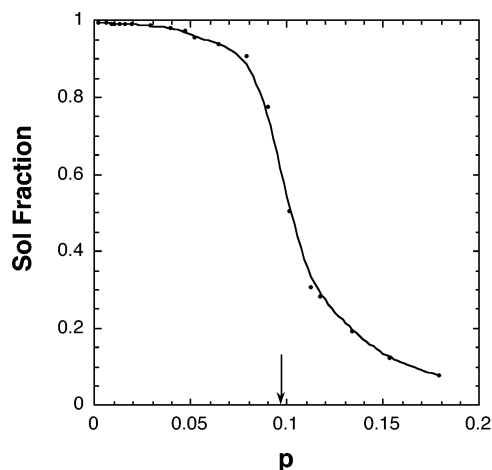


Figure 2. Sol fraction as a function of the conversion of reactive sites near the gel point. The arrow identifies our estimate of the gel point at $p = 0.096$.

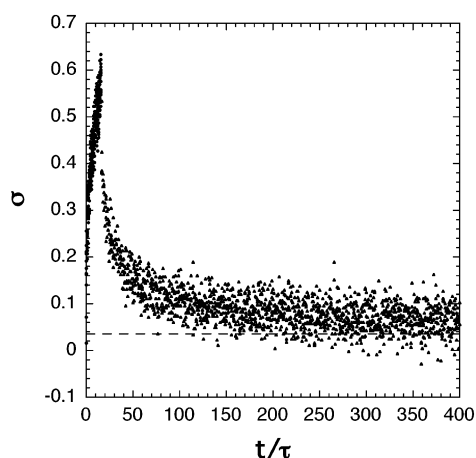


Figure 3. Time dependence of the stress (in units of ϵ/σ^3) of the network when the cross-linking is turned off and the sample is uniaxially deformed to $\lambda = 1.5$ ($0 \leq t \leq 16\tau$) and then allowed to relax ($15\tau \leq t \leq 400\tau$). Note that the stress has essentially reached a constant value after $t = 400\tau$.

The kinetics of the postcuring process are shown in Figure 1. Each of these networks was uniaxially stretched to $\lambda = 1.5$ over a time period of 16τ , allowed to equilibrate for 5000τ without additional reaction, after which the deviatoric stress σ was found by further averaging for an additional 5000τ . A typical stress relaxation curve is shown in Figure 3. It can be seen that after 400τ most of the stress has relaxed and σ is approximately constant. This quasi-equilibrium stress, normalized by $(\lambda^2 - 1/\lambda)$, is shown in Figure 4 as a function of $p - p_c$. As expected from rubber elasticity theory, we find that the uniaxial stress σ is a linear function of the number of cross-links which we expect to be proportional to $p - p_c$. We emphasize that this holds when all the cross-linking occurs in the unstrained state.

Now consider the stress response when the network is postcured in the strained state. For the same sample networks that were prepared above by cross-linking in the unstrained state, the reactions were turned off and the samples uniaxially deformed to $\lambda_1 = 1.5$ and then allowed to equilibrate for 10000τ . The cross-linking is then turned on in the strained state, and the deviatoric stress σ is then monitored as a function of conversion. According to the independent network hypothesis, no change in stress should be observed. The results of these

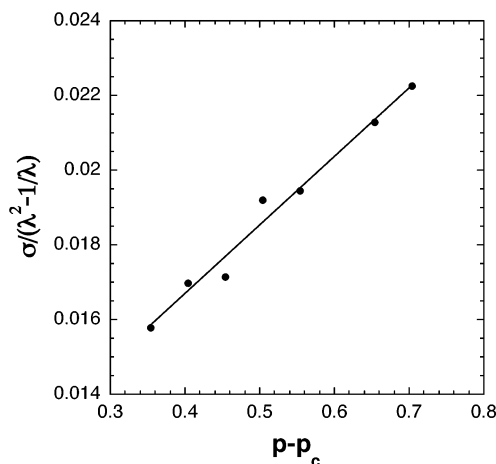


Figure 4. Normalized stress σ (in units of ϵ/σ^3) for samples cross-linked in the undeformed state to various conversions $p - p_c$. The stress was obtained after the network was deformed to $\lambda = 1.5$ and then allowed to relax.

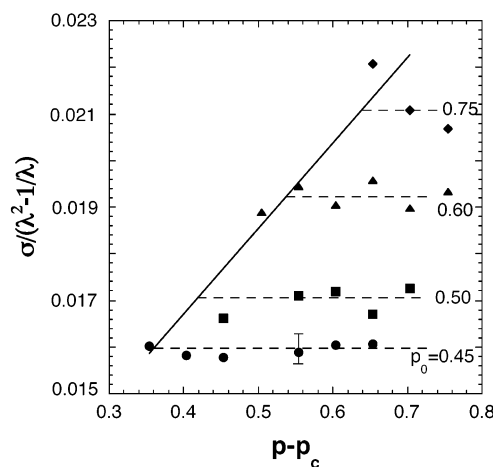


Figure 5. Normalized stress σ (in units of ϵ/σ^3) for networks cross-linked in the deformed state as a function of conversion $p - p_c$. The networks were initially reacted to various levels of conversion p_0 in the unstrained state. The networks were then deformed to $\lambda = 1.5$ and relaxed, after which the cross-linking reactions were again turned on. The estimated error bars are shown on one of the points. The solid line is the corresponding predictions from Figure 4 when all the cross-linking occurs in the undeformed state. The dashed lines are drawn as guides to the eye.

simulations are plotted in Figure 5 for various initial conversions p_0 ; it can be observed that the stress does not change within the estimated error of the stress calculation. For purposes of comparison, the stresses from uniaxially deformed networks, cross-linked in the unstrained condition, and deformed to $\lambda = 1.5$ (from Figure 4) are shown in Figure 5 as the solid line. It is obvious that additional cross-linking ν_1 in the deformed networks has very little or no effect on the stress compared to network chains ν_0 formed in the unstrained state. These results are general in the sense that no rubber elasticity model is invoked and are consistent with the independent network hypothesis.

The additional cross-linking in the strained state will be manifested as the permanent set the network experiences when the deviatoric stress is removed. To measure the permanent set, we systematically reduced the deformation ratio from $\lambda_1 = 1.5$ to λ_s and monitored the stress σ . Results are shown in Figure 6 for two networks that were initially deformed at $p = 0.45$. One sample

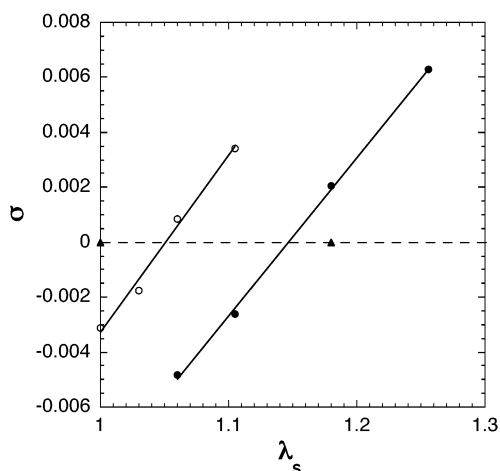


Figure 6. Stress (in units of ϵ/σ^3) on a network that has reacted to $p = 0.45$ in the undeformed state, reacted further to $p = 0.85$ (filled circles) in the deformed state $\lambda = 1.5$, and then released to various deformations λ_s shown. The open circles represent a control simulation where no additional cross-linking takes place in the deformed state. The permanent set is identified where the stress is interpolated to zero. The triangles are the predictions from eqs 6 and 7.

was postcured until $p = 0.85$, after which the reactions were turned off, while no postcuring occurred in the other sample. Three additional networks at $p = 0.65$, 0.75 , and 0.80 were also studied; although they are not shown in Figure 6, these results were intermediate as expected between the two extremes depicted in the figure. It can be seen that the stress varies approximately linearly with the new deformation ratio λ_s . From interpolation, we can identify the permanent set from the $p = 0.85$ network as $\lambda_s = 1.15$, corresponding to $\sigma = 0$. The equivalent prediction from the independent network model, together with the affine model for rubber elasticity, is $\lambda_s = 1.18$ and is also shown in Figure 6.

The network with $p = 0.45$ was the control sample. Since no cross-links are added in the strained state, it is expected to return to its original length ($\lambda_s = 1.0$) when released. It can be seen from Figure 6, however, that the MD result yields $\lambda_s = 1.05$. The failure of this network to completely recover in our simulations is probably due to residual viscoelastic effects that have not completely relaxed out over the strain history experienced by the network. This reveals the difficulties of extracting true equilibrium properties from MD simulations of networks. It should be added, however, that laboratory experiments are subject to similar limitations.

The permanent set P_s from the affine model calculated from eq 7 is plotted in Figure 7 as a function of v_1/v_0 for three different values of λ_1 . In these calculations we estimated v_1/v_0 from the fraction of active sites that have reacted to form cross-links according to

$$\frac{v_1}{v_0} = \frac{P_1 - P_0 - P_c}{P_0 - P_c} \quad (10)$$

From eq 7 we observe that $P_s = 0$ and 1 in the limits where $v_1/v_0 \rightarrow 0$ and ∞ , respectively. The permanent set from MD simulations of the five networks studied are shown as points in Figure 7. Note that $P_s \approx 0.1$ rather than 0.0 in our control sample because of viscoelastic effects. One would expect that similar effects would be

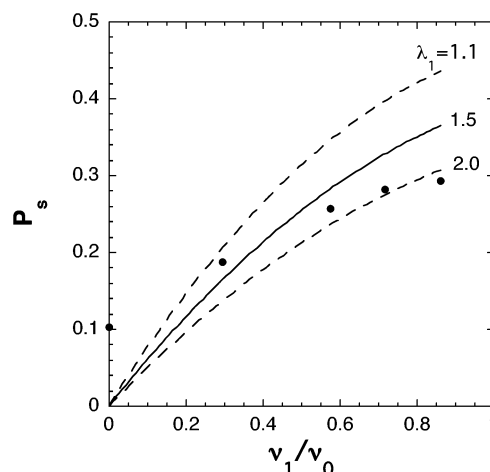


Figure 7. Permanent set predicted from the affine model in eq 7 as a function of the cross-linking ratio v_1/v_0 in the deformed and undeformed states for three values of λ_1 . The points represent the permanent set estimated from our MD simulations and should be compared with the solid curve where $\lambda_1 = 1.5$.

present in the other networks as well so that the true equilibrium permanent set values would be lower than shown in Figure 7. Thus, we conclude that the affine model predictions for permanent set are too high. This is not surprising since it is known that the affine model of rubber elasticity is not in quantitative agreement with either laboratory experiments²³ or computer simulations.^{17,19}

Other more accurate rubber elasticity models could be used with the independent network hypothesis, provided one knows how the model parameters depend on the cross-link density. The data and analysis presented here were restricted to the case of uniaxial deformation. The independent network/affine model can be generalized^{3,4} to three-dimensional strain fields with deformations $\lambda_x, \lambda_y, \lambda_z$ in the principal directions by employing a strain energy function $W(\lambda_x, \lambda_y, \lambda_z)$. For the case of the affine model we have²³

$$W(\lambda_x, \lambda_y, \lambda_z) = \frac{\nu k_B T}{2V} (\lambda_x^2 + \lambda_y^2 + \lambda_z^2 - 3) \quad (11)$$

The stresses $\sigma_x, \sigma_y, \sigma_z$ in the principal directions are then given by

$$\sigma_i = \lambda_i \frac{\partial W}{\partial \lambda_i} = L_i \frac{\partial W}{\partial L_i} \quad (12)$$

subject to the incompressibility constraint that $\lambda_x \lambda_y \lambda_z = 1$. From the independent network hypothesis, we propose that the affine strain energy function can be generalized to incorporate the cross-linking/strain history by analogy with eq 3.

$$W(L_x, L_y, L_z) = \frac{k_B T}{2V} \int_{t_{\text{gel}}}^t \left[\left(\frac{L_x(t)}{L_x(s)} \right)^2 + \left(\frac{L_y(t)}{L_y(s)} \right)^2 + \left(\frac{L_z(t)}{L_z(s)} \right)^2 - 3 \right] \frac{dv}{ds} ds \quad (13)$$

Equations 12 and 13 could then be applied to predict the stress response to a network undergoing cross-linking reactions in a three-dimensional strain field.

V. Conclusions

In this investigation we used MD simulations of networks undergoing cross-linking reactions to test two

predictions of the independent network hypothesis first proposed by Tobolsky.¹ When cross-links are added to an undeformed polymer network, the uniaxial Young's modulus increases with cross-link density as expected from rubber elasticity theory. However, we found that when cross-links are added to a network held at a fixed uniaxial deformation, the stress did not change with cross-link density in accordance with the independent network hypothesis. This provides a general test because no additional assumptions are made. When the uniaxial stress is removed from our sample network, the network did not return to its initial length and a permanent set was observed. A nonzero permanent set is also a general consequence of the independent network hypothesis.

Using the independent network hypothesis, together with the affine rubber elasticity model, a constitutive equation was constructed (eq 3) to predict the uniaxial stress of a network for an arbitrary cross-link density/deformation history. The uniaxial permanent set prediction in eq 7 based on the affine model was found to predict higher permanent sets than observed in our MD simulations. Although a plausible extension of the independent network model to three dimensions has been carried out,^{3,4} further validation should be carried out in more general strain fields.

In this paper and in the original Tobolsky work¹ the affine model of rubber elasticity was used. Because of the well-known deficiencies of this model, it is likely that the discrepancy between the predicted and simulated permanent set is due to the rubber elasticity model and not the independent network approximation. It would be worthwhile to employ a more accurate rubber elasticity theory with the independent network approximation to deduce a more accurate constitutive model than given in eq 13. It should be pointed out, however, that the phantom network model of James and Guth,³⁰ where network junctions are completely free to fluctuate, would also lead to the same permanent set as in eq 7. This is because in both the affine and phantom models the stress has the same deformation dependence, and the models only differ in the coefficients. A more accurate permanent set prediction would possibly arise from the Mooney–Rivlin²³ equation, constrained-junction theories,^{31,32} tube models,³³ or more recent non-affine models.^{28,34} Mott and Roland⁹ recently performed permanent set calculations based on a constrained junction model.

Finally, it should be mentioned that our simulations used a coarse-grained, bead–spring model description of a polymer network. In this model the average bond length is close to the nearest-neighbor distance between monomers in the bulk liquid. Thus, when a cross-link is formed from a pair of nearby monomers, the monomer/monomer distance does not change appreciably. Hence, the network does not undergo significant volumetric shrinkage. This may not be the case for a more atomistic model where bond lengths are typically smaller than

the site diameters. In cases where there is appreciable shrinkage during cross-linking one might expect the independent network hypothesis to break down.

Acknowledgment. Sandia is a multiprogram laboratory operated by Sandia Corporation, a Lockheed Martin Company, for the United States Department of Energy's National Nuclear Security Administration under Contract DE-AC04-94AL85000.

References and Notes

- (1) Tobolsky, A. V. *Properties and Structure of Polymers*; Wiley: New York, 1960.
- (2) Andrews, R. D.; Tobolsky, A. V.; Hanson, E. E. *J. Appl. Phys.* **1946**, *17*, 352.
- (3) Berry, J. P.; Scanlan, J.; Watson, W. F. *Trans. Faraday Soc.* **1956**, *52*, 1137.
- (4) Flory, P. J. *Trans. Faraday Soc.* **1960**, *56*, 722.
- (5) Curro, J. G.; Salazar, E. A. *J. Appl. Polym. Sci.* **1975**, *19*, 2571; *Rubber Chem. Technol.* **1977**, *50*, 895.
- (6) Salazar, E. A.; Curro, J. G.; Gillen, K. T. *J. Appl. Polym. Sci.* **1977**, *21*, 1597.
- (7) Tobolsky, A. V.; Prettyman, I. B.; Dillon, J. H. *J. Appl. Phys.* **1944**, *15*, 380.
- (8) Huntley, H. E.; Wineman, A. S.; Rajagopal, K. R. *IMA J. Appl. Math.* **1997**, *59*, 309. Wineman, A. S.; Rajagopal, K. R. *Arch. Mech.* **1990**, *42*, 53. Rajagopal, K. R.; Wineman, A. S. *Int. J. Plast.* **1992**, *8*, 385.
- (9) Mott, P. H.; Roland, C. M. *Macromolecules* **2000**, *33*, 4132.
- (10) Santangelo, P. G.; Roland, C. M. *Rubber Chem. Technol.* **2003**, *76*, 892.
- (11) Leung, Y. K.; Eichinger, B. E. *J. Chem. Phys.* **1984**, *18*, 983.
- (12) Shy, L. Y.; Leung, Y. K.; Eichinger, B. E. *Macromolecules* **1985**, *80*, 3877.
- (13) Shy, L. Y.; Eichinger, B. E. *Br. Polym. J.* **1985**, *17*, 200.
- (14) Galiatsatos, V.; Eichinger, B. E. *J. Polym. Sci.* **1988**, *26*, 595; *Rubber Chem. Technol.* **1988**, *62*, 205.
- (15) Shy, L. Y.; Eichinger, B. E. *Macromolecules* **1986**, *19*, 2787.
- (16) Everaers, R.; Kremer, K. *Macromolecules* **1995**, *28*, 7291; *Phys. Rev. E* **1996**, *53*, R37.
- (17) Mergell, B.; Everaers, R. *Macromolecules* **2001**, *34*, 5675.
- (18) Svaneborg, C.; Grest, G. S.; Everaers, R. *Phys. Rev. Lett.*, submitted for publication.
- (19) For a review see: Everaers, R. *New J. Phys.* **1999**, *1*, 12.1.
- (20) Grest, G. S.; Kremer, K. *J. Phys. (Paris)* **1990**, *51*, 2829; *Macromolecules* **1990**, *23*, 4995.
- (21) Duering, E. R.; Kremer, K.; Grest, G. S. *Macromolecules* **1993**, *26*, 3241; *J. Chem. Phys.* **1994**, *101*, 8169.
- (22) Grest, G. S.; Kremer, K.; Duering, E. R. *Physica A* **1993**, *194*, 330.
- (23) Treloar, L. R. G. *The Physics of Rubber Elasticity*; Clarendon Press: Oxford, 1975.
- (24) Ellul, M. D.; Southern, F. *Plast., Rubber Compos. Process. Appl.* **1985**, *5*, 61.
- (25) Plimpton, S. J. *Comput. Phys.* **1995**, *117*, 1.
- (26) Kremer, K.; Grest, G. S. *J. Chem. Phys.* **1990**, *92*, 5057.
- (27) Auhl, R.; Everaers, R.; Grest, G. S.; Kremer, K.; Plimpton, S. J. *J. Chem. Phys.* **2003**, *119*, 12718.
- (28) Everaers, R. *Eur. J. Phys. B* **1998**, *4*, 341.
- (29) Rubinstein, M.; Colby, R. H. *Polymer Physics*; Oxford University Press: Oxford, 2003.
- (30) James, H. M.; Guth, E. *J. Chem. Phys.* **1943**, *11*, 455.
- (31) Ronca, G.; Allegra, G. *J. Chem. Phys.* **1975**, *63*, 4990.
- (32) Erman, B.; Flory, P. J. *J. Chem. Phys.* **1978**, *68*, 5363.
- (33) Edwards, S. F.; Vilgis, T. A. *Rep. Prog. Phys.* **1988**, *51*, 243.
- (34) Rubinstein, M.; Panyukov, S. *Macromolecules* **1997**, *30*, 8036.

MA049723J